Investigating the applicability of surface models for laser scanner-based deformation analysis

Lina STAUSBERG[1,*], **Nils QUADT**[1], **Berit JOST**[1], and **Heiner KUHLMANN**[1]

[1] *University of Bonn, Bonn, Germany, (stausberg@igg.uni-bonn.de, s7niquad@uni-bonn.de, b.jost@igg.uni-bonn.de, heiner.kuhlmann@uni-bonn.de)*

[*] *corresponding author*

Abstract

Germany has over 300 dams that require regular stability inspections through geodetic deformation measurements and analysis. This process typically relies on fixed object points, marked by pillars, elevation bolts, or targets placed near and on the dam wall. A two-epoch comparison then reveals any point deformations. For research purposes, area-based deformation analysis of dams are increasingly performed using terrestrial laser scans. This approach allows for the examination of the entire airside surface of the dam, rather than just individual points. Creating 3D models of this surface can be an effective tool for assessing the stability of the dam. Therefore, it is crucial to evaluate which methods are best suited for generating such 3D models to detect potential deformations. Within the study, we investigate different methods for surface reconstruction and develop a working program to use these models for deformation analysis. First, we will investigate the applicability of different reconstruction methods to our data and then analyse the advantages and disadvantages of these methods with respect to deformation analysis.

Keywords: deformation monitoring, terrestrial laser scanner, surface modelling

1 Introduction

There are more than 300 large dams in Germany (DTK, 2013). According to DIN 19700 "Stauanlagen", each dam must undergo an annual stability inspection. These inspections are based on geodetic deformation measurements and subsequent analysis. For this purpose, a geodetic network of fixed points and object points is established at the dam. Pylons, levelling bolts and other targets are attached to the dam wall and measured using tachymetric methods. Stability assessments are made by comparing data from two measurement epochs. Traditional tachymetric methods analyse movement by identifying changes in individual points between these epochs, thereby simplifying the deformation of the dam to a limited set of measurement points.

In recent years, terrestrial laser scanners (TLS) have emerged as an innovative measurement system capable of efficiently scanning large areas. TLS generates high-resolution point clouds that allow deformation analysis not only for selected points, but also for the entire air-facing surface of the dam wall. The Cloud-to-Cloud (C2C) method allows direct comparison of point clouds from different epochs, although it is computationally intensive. Alternatively, 3D models can be generated from point clouds. These models can then be compared using mesh-to-mesh (M2M) methods or with the original point clouds using cloud-to-mesh (C2M) analysis.

In the following we will investigate two different surface reconstruction methods and evaluate which of these methods is more suitable for modelling the dam wall. We will then test and compare the resulting models for their applicability in the context of deformation analysis. Finally, we will compare our method with established methods and analyse whether or not our method is better suited for this application.

2 Data

For our investigation we use data measured from the Jubach water dam, located in the municipality of

Kierspe in North Rhine-Westphalia (see figure 1). It was constructed between 1904 and 1906. The dam has a crest length of 152m and rejuvenates with a foundation thickness of 19.2m to a crest width of 4.5m with a total height of 27.5m. The capacity of the Jubach Dam is $1.05 \cdot 10^6 m^3$ with a maximum surface area of 11.7ha (Structurae, 2024). The dam wall, made of quarry stone, belongs to the class of gravity dams. Between 1990 and 1991 it was reinforced and sealed with a reinforced concrete sealing wall.

Figure 1. Jubach dam photographed with a drone from the land side.

The data used was acquired using a Leica ScanStation. The point cloud results from two-layer observations of the dam wall with a resolution of 3.2mm at 10m. The targets were also acquired with a resolution of 0.8mm at 10m. This is a point cloud taken from a point where the entire airside is visible. As a last step the point cloud was georeferenced using the Software *Cyclone*.

3 Methods

In the following chapter we will summarize the methods used to create a surface model out of the point cloud. In section 3.1 we will describe the preprocessing steps needed before the reconstruction and in sections 3.2 and 3.3 the different methods to create the surface model are described.

3.1 Preprocessing

After the data acquisition, the point cloud still contains relatively many parts that are irrelevant for our further investigation (ground points, vegetation in front of the wall and rough outliers), so it needs to be cleaned up before reconstruction. The first step is to remove the coarse outliers and uninteresting parts from the point cloud. This is done by first reducing the number of points and then manually removing ground and vegetation points. To reduce the number of points, a downsampling of the whole point cloud is performed, setting the average distance between the points to 1cm. In figure 2 the preprocessed point cloud is shown, which later is used for the reconstruction methods.

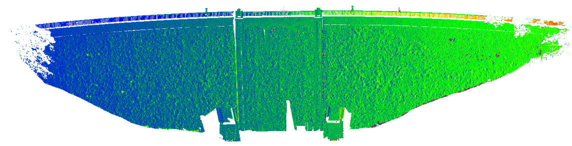

Figure 2. Example point cloud of the Jubach water dam after preprocessing.

3.2 Ball-Pivoting Algorithm

As one option, we use the ball-pivoting algorithm (Bernardini et al., 1999) to reconstruct the dam surface. This method efficiently generates a triangular mesh from a dense point cloud.

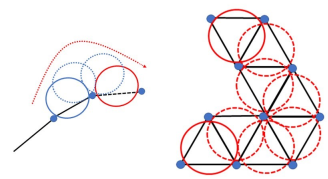

Figure 3. Visualization of the ball rotation algorithm presented in Bernardini et al. (1999).

The algorithm begins by placing a virtual ball of radius ρ in contact with three points that form a seed triangle. While maintaining contact with two of these points, the ball pivots until it touches a third point, forming a new triangle. Repeating this process along the edges of the mesh produces a continuous triangle mesh. See figure 3 for an illustration.

3.3 Poisson Surface Reconstruction

Another option to generate a closed, triangulated surface from point cloud data is the Poisson surface reconstruction (Kazhdan et al., 2006). This method requires input points, denoted as s_p, along with associated point normals s_N oriented inwards towards the object. Since laser scanners typically do not provide normal information, these normals must first be estimated using the K-nearest-neighbour algorithm combined with the least squares method.

The aim of this technique is to construct an indicator function χ_M that determines whether a given

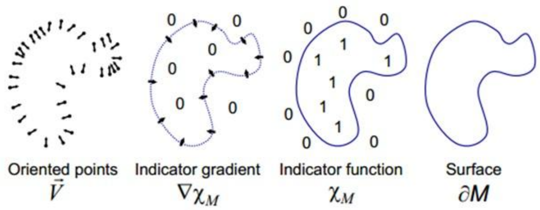

Figure 4. Illustration of the Poisson reconstruction in 2D.(Kazhdan et al., 2006)

point is inside or outside the object. The relationship between the oriented points and the indicator function is expressed by integrals. The gradient of the indicator function, $\nabla\chi_M$, forms a vector field $\overrightarrow{V}$ that is aligned with the point normals on the surface. To achieve this, the process involves solving for a scalar function χ_M that best approximates the vector field V by minimising the difference (see figure 4 for an illustration). This optimisation problem is governed by the Poisson equation:

$$\min_{\chi_M} \|\nabla\chi_M - \overrightarrow{V}\|. \tag{1}$$

3.4 Point cloud comparison

The reconstructed surfaces are used to perform an areal deformation analysis of a dam wall using the surface models. Traditionally, deformation analysis is carried out using a 2-epoch comparison where individual points are checked for deviations (Möser et al., 2000). For point clouds, however, this approach is only possible if identical points are extracted from the clouds, which requires identical locations and angular resolutions of the laser scanners in both measurement epochs (Holst et al., 2016). Alternatively, point cloud comparisons can be used to analyse differences between two states, as described in the following subsection. The aim is to determine whether deformation has occurred on the target object and to determine its magnitude and direction.

3.4.1 Cloud-to-Mesh comparison (C2M)

Cloud to mesh (C2M) is a method of comparing a point cloud to a global mesh. Distances between the mesh and the point cloud are calculated by determining the closest point to each mesh. This standard approach works well for flat surfaces, but is less suitable for rough surfaces with data gaps due to the high computational cost (Lague et al., 2013).

The triangulations created by using the beforehand mentioned surface reconstruction methods are used for comparison. The normal vectors of the meshes are used to calculate the distances between the meshes and the point cloud. Random deviations and noise in the point cloud can complicate the interpretation of the results (Holst et al., 2016). As with the cloud-to-cloud (C2C) comparison, the result is presented as a colour-coded point cloud visualising the distances to the surface.

3.4.2 Mesh-to-Mesh comparison (M2M)

As a further example of surface based methods, a comparison can be made between two meshing methods. As with the C2M comparison, the shortest distances between the two surfaces are determined. As the normal vectors always reflect the direction of the shortest connection between two surfaces, they are calculated in each case. Finally, the magnitude of the normal vectors reflects the distance between the two surface models. Although an M2M comparison can be calculated in CloudCompare, only the nodes from the reference mesh are used for the comparison (Holst et al., 2016). This means that the implementation of M2M in MATLAB is a C2M comparison using the nodes of the mesh.

3.5 Deforming the point cloud

In order to study deformation under controlled conditions, a deformed data set must first be generated and analysed. Dams exhibit water level-dependent movements that only become dangerous when a critical value is exceeded, necessitating measures such as evacuation. Holst et al. (2017) point out that small-scale deviations of around one centimetre due to water level fluctuations are common.

For the analysis, a simulated deformation of the dam wall of eight to ten millimetres is modelled, as the largest movement occurs in the central area of the dam wall at full water level. The deformation is described by a rotation around the x_2-axis with the rotation matrix:

$$R = \begin{bmatrix} \cos(-0.02^\circ) & 0 & \sin(-0.02^\circ) \\ 0 & 1 & 0 \\ -\sin(-0.02^\circ) & 0 & \cos(-0.02^\circ) \end{bmatrix} \tag{2}$$

The central area of the dam is extracted from the point cloud in CloudCompare, the rotation is applied and the partial point clouds are merged again. Finally, meshing is performed using the BPA and Poisson methods.

4 Results

In the following section, we will apply the previously mentioned reconstruction methods to our Jubach water data, starting with the Ball-Pivoting algorithm in section 4.1 and then using the Poisson surface reconstruction in section 4.2. In the last section 4.3 we use the reconstructed surfaces for a deformation analysis.

4.1 Ball-Pivoting

For modelling with Ball-Pivoting algorithm (BPA), appropriate ball radii are determined empirically based on local point spacing. In figure 5 an example for the reconstruction of a test region can be seen. The high point density in both regions indicates good meshing results. Initially, BPA uses radii ρ of 0.5, 1.0 and 1.5cm (5a), applied adaptively, but some holes remain despite the points available. Adding twice the point spacing significantly improves model closure (5b).

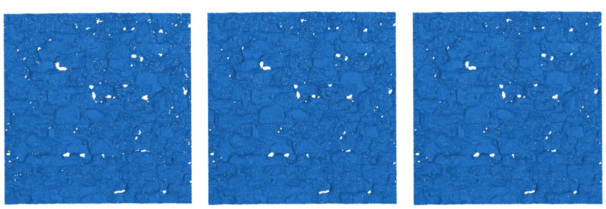

(a) (b) (c)

Figure 5. BPA in area 1 of the dam wall with different ball radii: (a) $\rho = [0.5, 1.0, 1.5]$ [cm], (b) $\rho = [0.5, 1.0, 1.5, 2.0]$ [cm] and (c) $\rho = [0.5, 1.0, 1.5, 2.0, 2.5, 5.0]$ [cm].

Using the full point cloud reveals holes in the dam's outer region due to low point density, increased spacing and shadowing from rough surfaces. To address this, radii are adjusted using $\rho = [0.5, 1.0, 1.25, 1.5, 2.5, 5] \cdot d$, where d is the average point distance which is set to 1cm in pre-processing.

Figure 6 shows the reconstruction, which retains some holes but provides a high level of detail. BPA ends the triangulation at the edges of the dam, the remaining holes, mostly on the sides, are due to low point density. Larger radii could close them, but would reduce accuracy. Reducing the holes will require multiple scan points and combined registration.

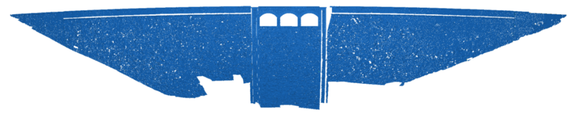

Figure 6. Reconstruction result of the whole dam using $\rho = [0.5, 1.0, 1.25, 1.5, 2.5, 5]$ [cm]

4.2 Poisson Surface Reconstruction

For the Poisson reconstruction we start with smaller test regions. The algorithm reliably triangulates the point cloud in the first region (figure 7a). In the flood overflow area (figure 7b), the Poisson method closes openings as it aims to create a closed model, resulting in extensions beyond the point cloud.

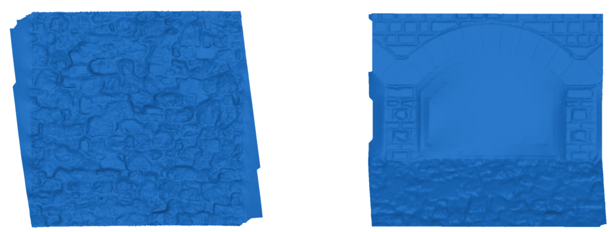

(a) (b)

Figure 7. The mesh of the Poisson reconstruction (with octree depth = 8) in two example areas of the whole point cloud. The area in (a) is centred on the central part of the point cloud, while area (b) shows the flood overflows.

The level of detail can be controlled by adjusting the octree depth. For the test areas in figure 7 a high level of detail is achieved. However, meshing the entire point cloud with an octree depth of 8 results in excessive smoothing (figure 8a), while increasing the depth to 12 improves the results (figure 8b). The reconstruction always extends surfaces beyond the point cloud boundaries, regardless of the octree depth. This is because the Poisson method attempts to create a closed model. These areas, which could distort the deformation analysis, are removed.

The model reliably closes data gaps (figure 8b), but distinguishes between intentional gaps, such as flood overflows, and unintentional gaps caused by shadowing (figure 9). The Poisson method approximates missing regions, such as the transition between the central flood spillway and the right dam section (figure 9), using distant neighbouring points. This should be taken into account in the deformation analysis.

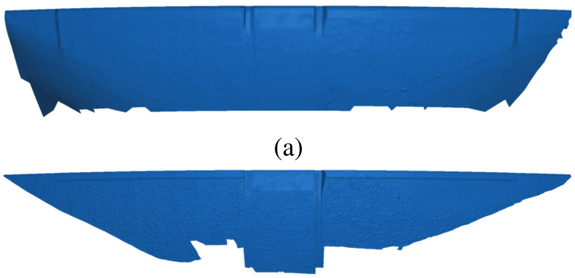

(a)

(b)

Figure 8. (a) Mesh created with the Poisson surface reconstruction and an octree depth of 8. (b) Mesh created with the Poisson surface reconstruction and an octree depth of 12.

The model generally shows a high level of detail, especially in areas of high point density. The joints between the quarry stones of the dam are also visible. However, the model reconstructed using the Poisson method is significantly smoother than the mesh using the BPA. As a result, the structure of the wall is not visible in the model. Individual bricks cannot be resolved.

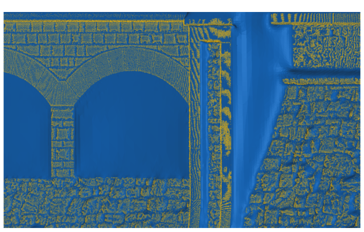

Figure 9. Zoom into the surface model. The surface model is depicted in blue, while the original point cloud is shown in yellow.

4.3 Deformation Analysis

So far, different meshing methods have been calculated based on the point cloud of the Jubach Dam. The next step is to perform a deformation analysis to assess which reconstruction method is better suited for deformation analysis. As only one point cloud from one epoch is available, a simulated deformed dataset is first generated (Section 3.5) and then analysed.

Two approaches are considered for the deformation analysis: the cloud-to-mesh (C2M) comparison and the mesh-to-mesh (M2M) comparison. The focus here is on the suitability of the meshes rather than the point clouds.

4.3.1 Cloud-to-Mesh comparison (C2M)

The point cloud comparison C2M is used to compare the models calculated from the laser scan data of the Jubach dam with the deformed point cloud of the dam. After selecting the mesh as the reference and the point cloud as the comparison object, the point cloud comparison calculation is started. The comparison is then made between the surface obtained from the BPA modelling and the deformed point cloud, and then between the surface reconstructed using the Poisson method and the deformed point cloud.

Figure 10 shows the result of the C2M comparison of the original point cloud and the model of the deformed point cloud generated by the BPA. Here, figure 10a shows the result of the C2M comparison directly on the dam data and figure 10b shows the corresponding histogram. Firstly, it can be clearly seen that the deformation described above is successfully detected. The deformation values obtained are in line with the expected values. Note that the C2M distances to be displayed were set to the interval $[-0.01\text{m}, 0.01\text{m}]$. This will also be used for the following C2M and M2M comparisons to ensure comparability.

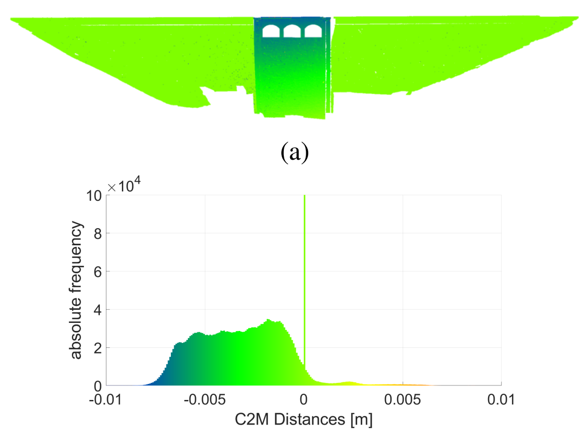

(a)

(b)

Figure 10. (a) Result of the C2M with the mesh from the BPA as reference and the deformed point cloud as comparison object. (b) Corresponding histogram over the C2M distances.

The dam is divided into three sections: left, middle and right, with deformation occurring in the middle section (see Fig. 10a). Some anomalies are also observed in the left and right sections due to holes in the mesh. These gaps in the triangulation cause nearby points from the deformed point cloud to fall within the significant range of one centimetre. However, as only a few points are affected, the overall C2M comparison with the BPA model remains positive.

The histogram in figure 10b shows a shift towards negative values. This is because the deformed mesh is used as a reference, reversing the previously applied positive deformation. There is also a narrow peak at distance 0, which is expected as only the central part of the point cloud has been deformed.

For the Poisson surface reconstruction (Fig. 11), the C2M result similarly highlights the central deformation but shows significantly more noise compared to the BPA mesh. The joints between the quarry stones and the transitions between the central, left and right sections of the dam are particularly noticeable.

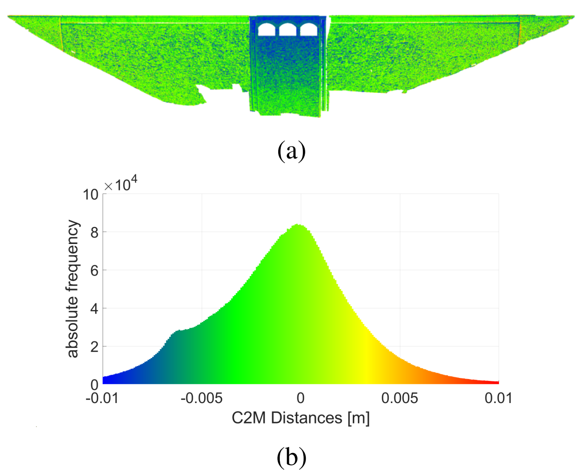

Figure 11. (a) Result of the C2M with the mesh from the Poisson mesh as reference and the deformed point cloud as comparison object. (b) Corresponding histogram over the C2M distances.

The reason for this is that the Poisson mesh does not pass directly over the individual points in the point cloud, but between them. This also makes it possible to identify areas of the dam where offsets occur. These show deviations with a positive sign in the C2M comparison (see figure 11a). In summary, the artificially generated deformation of the point cloud can be detected with both reconstruction methods. However, the C2M comparison with the Poisson model shows additional movement in other areas that were not modified.

Comparing the histograms in the figures 10b and 12b, it can be seen that there is significant noise in the C2M when using the Poisson method. It can also be seen that the C2M deviations are larger when using the Poisson reconstruction than when using the BPA. The distances are more scattered in the histogram and are also below and above one centimetre in both directions.

4.3.2 Mesh-to-Mesh comparison (M2M)

The point cloud comparisons between the models are calculated below. The M2M comparison is carried out for both the BPA mesh and the Poisson mesh. Figure 12 shows the result for the BPA model, while figure 13 shows them for the Poisson model. For the BPA model, the simulated deformation is reliably detected by the M2M comparison and is confined to the central area of the point cloud (see 12a). There is no difference in the lateral areas of the dam. Isolated displacements occur only in transition areas with lower point density.

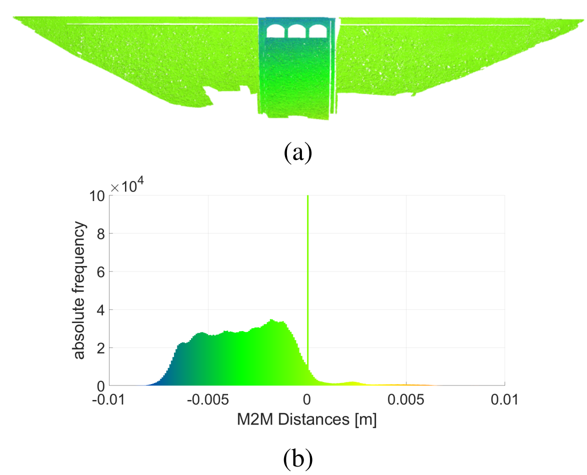

Figure 12. (a) Result of the M2M comparison using the meshes of the original an the deformed point cloud generated with the BPA. (b) Corresponding histogram over the M2M distances.

Figure 12b shows the histogram of the M2M comparison and a strong similarity between this histogram and the histogram of the C2M comparison (figure 10b) can be seen. This is due to the fact that CloudCompare actually computes a C2M comparison in the M2M comparison, which is based on the interpolation points of the models. As these support points fall on the points of the point cloud due to the interpolative approach, the results are similar. The positive deviations previously detected in the C2M comparison in the edge areas of the dam wall are no longer detected here as the mesh is identical there.

The deformation is also detected in the Poisson model (figure 13a), but large deviations occur in the data gaps as the Poisson method attempts to close these areas. The largest differences can be seen at the flood spillways and the transitions between the centre and side elements of the dam. In addition, offsets with a positive sign can be seen. The truncation of the overhangs also results in differences at the edges of the model.

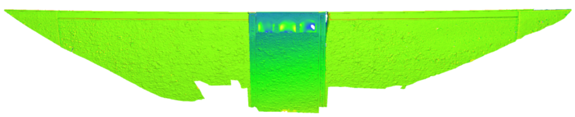

(a)

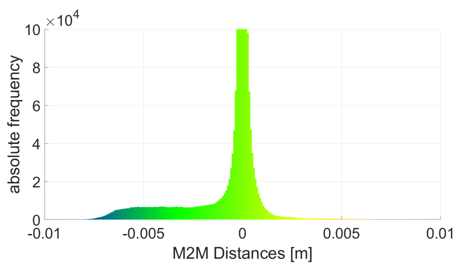

(b)

Figure 13. (a) Result of the M2M comparison using the meshes of the original an the deformed point cloud generated with the Poisson Method. (b) Corresponding histogram over the M2M distances.

The histogram in figure 13b shows the M2M comparison between the undeformed and deformed Poisson model. The deformation is less obvious here than in the BPA mesh as there are fewer points in the area of maximum deformation. In addition, the maximum has a wider spread, making the undeformed area larger and less clearly defined.

5 Discussion

The results of the reconstruction methods and point cloud comparisons (C2M and M2M) are summarised and discussed below. Overall, the simulated deformation was reliably detected in both the Ball-Pivoting algorithm and Poisson meshes, although clear differences are visible.

The intentionally small rotation angle of -0.02° was used to check whether even minimal deformations could be detected. BPA maps the point cloud accurately using triangles, while the Poisson method produces a smooth surface between the points and does not provide an accurate point reconstruction. The BPA mesh has a high level of detail, but with individual holes. On the positive side, flood spillways are preserved as such, whereas the Poisson method attempts to create a closed model, often beyond the point cloud. The choice of octree level affects the level of detail: too high values result in angular surfaces, too low in smoothed surfaces.

The different objectives of the meshing methods lead to deviations in the point cloud comparisons. Artefacts occur in the C2M comparison of the Poisson model, such as visible joints between quarry stones and offsets in the dam wall. As the Poisson method smooths and does not interpolate accurately, reliable deformation analysis is difficult. In comparison, C2M with BPA mesh gives better results. Although local deviations do occur, they are less frequent than with the Poisson model. These are caused by insufficient point density, which could be remedied by larger sphere radii or additional scans. Overall, the BPA reconstruction is better at detecting artificial deformations with high point density.

The M2M comparison, shows a similar picture. With the BPA mesh, the deformation is reliably detected, while no deviations occur in the unaffected edge areas. Only at the transitions to the deformed area do distances appear due to the low point density. The histogram of the BPA-C2M comparison confirms these results and is similar to that of the M2M. The M2M comparison between the deformed and non-deformed Poisson model shows the deformation, but there are significant deviations at the transitions of the dam parts and the flood overflows, well above the limit of one centimetre. As the Poisson method always generates a closed triangular mesh, these areas are closed even though no observations are available there. This leads to large deviations between the meshes. There are also artefacts at the intersections due to the cutting of the meshes. The deformation is less obvious in the histogram than for the BPA meshes.

In terms of run times (table 1), the deformation analysis using the C2M and M2M comparisons are significantly longer than the analysis based on the Poisson models when using the meshes generated according to the BPA. The mean point distances (table 1) are very similar for all methods and differ only in the sub-millimetre range.

Table 1. Runtimes and results of the C2M and M2M point cloud comparisons on the Jubach water dam data set.

Method	Runtime [s]	σ [mm]
C2M BPA	82.42	2.6
C2M Poisson	27.68	4.5
M2M BPA	82.42	1.9
M2M Poisson	14.93	1.9

Finally, CloudCompare also provides an empirical standard deviation (table 1) for the results of the point cloud comparisons. It is noticeable that it is lowest for the M2M method in combination with the BPA mesh. Although the values for the M2M comparison of the Poisson models are even lower, this is due to the settings made in CloudCompare. These are set so that areas in the result plots that are outside the maximum distance to be displayed are not coloured grey.

6 Conclusion and Outlook

The aim was to investigate whether potential deformation could be detected in the model of the dam. Two reconstruction methods were investigated: the triangulating ball pivoting algorithm (BPA) and the smoothing Poisson method. The quality of the model could be influenced by adjusting the ball radius in the BPA and the octree depth in the Poisson method.

The BPA mesh produced a high level of detail but with holes, while the Poisson model produced closed, smoothed surfaces. An artificial displacement of about one centimetre was introduced for deformation analysis. All methods were able to detect this, with the M2M comparison with BPA providing the most reliable results. The Poisson method showed greater deviations in the unaltered areas.

In the future, it would be useful to test BPA with more densely sampled point clouds and to develop statistically sound methods for dam monitoring. It would also be useful to test the M2M comparison in programmes that support real area comparisons.

Acknowledgements

This work was funded by the Deutsche Forschungsgemeinschaft (DFG, German Research Foundation) under Germanys Excellence Strategy - EXC 2070-390732324.

References

Bernardini, F., Mittleman, J., Rushmeier, H., Silva, C., and Taubin, G. (1999). The ball-pivoting algorithm for surface reconstruction. *IEEE transactions on visualization and computer graphics*, 5(4):349–359.

DTK (2013). *Talsperren in Deutschland*. Springer Fachmedien Wiesbaden.

Holst, C., Schmitz, B., and Kuhlmann, H. (2016). Tls-basierte deformationsanalyse unter nutzung von standardsoftware. *Terrestrisches Laserscanning*.

Holst, C., Schmitz, B., Schraven, A., and Kuhlmann, H. (2017). Eignen sich in Standardsoftware implementierte Punktwolkenvergleiche zur flächenhaften Deformationsanalyse von Bauwerken? Eine Fallstudie anhand von Laserscans einer Holzplatte und einer Staumauer. *ZfV-Zeitschrift für Geodäsie, Geoinformation und Landmanagement*, (zfv 2/2017).

Kazhdan, M., Bolitho, M., and Hoppe, H. (2006). Poisson surface reconstruction. In *Proceedings of the fourth Eurographics symposium on Geometry processing*, volume 7.

Lague, D., Brodu, N., and Leroux, J. (2013). Accurate 3d comparison of complex topography with terrestrial laser scanner: Application to the rangitikei canyon (nz). *ISPRS journal of photogrammetry and remote sensing*, 82:10–26.

Möser, M., Müller, G., Schlemmer, H., Heunecke, O., Kuhlmann, H., Welsch, W., Eichhorn, A., and Neuner, H. (2000). Auswertung geodaetischer überwachungsmessungen.

Structurae (2024). Internationale datenbank und galerie für ingenieurbauwerke. `https://structurae.net/de/bauwerke/jubachtalsperre`. Accessed: (03.02.2025).